Hierarchical Robust Control of Oscillating Wave Energy Converters With Uncertain Dynamics

Francesco Fusco, *Member*, *IEEE*, and John V. Ringwood, *Senior Member*, *IEEE*

***Abstract*—Energy-maximizing controllers for wave energy devices are normally based on linear hydrodynamic device models. Such models ignore nonlinear effects which typically manifest themselves for large device motion (typical in this application) and may also include other modeling errors. The effectiveness of a controller is, in general, determined by the match between the model the controller is based on and the actual system dynamics. This match becomes especially critical when the controller is highly tuned to the system. In this paper, we present a methodology for reducing this sensitivity to modeling errors and nonlinear effects by the use of a hierarchical robust controller, which shows small sensitivity to modeling errors, but allows good energy maximization to be recovered through a passivity-based control approach.**

***Index Terms*—Internal model control (IMC), passivity, robust control, wave energy conversion (WEC).**

Nomenclature

$n(t), N(\omega)$	Fourier transform pair.
$x(t)$	Heaving position of floating body.
$v(t)$	Heaving velocity of floating body.
$f_{\rm ex}(t)$	Wave excitation force.
$f_u(t)$	Power take-off force (control input).
$f_v(t)$	Viscous force.
$Z_i(\omega)$	Intrinsic impedance of floating system.
$B(\omega)$	Radiation resistance of floating system.
$K_v^{(0)}$	Linear approximation of viscous damping.
$1/H$	Ratio velocity to excitation force.
$X_{\rm lim}$	Constraint on heaving position.
$K_{\rm SG}(s)$	Feedback controller based on small-gain.
$K_{\rm SPR}(s)$	Feedback controller based on passivity.
H_s	Significant wave height.
ω_0	Peak frequency.
λ	Sharpness of Ochi standard spectrum.
PTO	Power take-off.
RCW	Relative capture width.
WEC	Wave energy converter.

Manuscript received November 02, 2013; revised February 17, 2014; accepted March 21, 2014. Date of publication April 22, 2014; date of current version June 17, 2014.

F. Fusco is with the Smarter Cities Technology Centre, IBM Research Ireland, Mulhuddart, Dublin 15, Ireland (e-mail: francfus@ie.ibm.com).

J. V. Ringwood is with the Centre for Ocean Energy Research, National University of Ireland Maynooth, Maynooth, County Kildare, Ireland (e-mail: john.ringwood@eeng.nuim.ie).

Color versions of one or more of the figures in this paper are available online at http://ieeexplore.ieee.org.

Digital Object Identifier 10.1109/TSTE.2014.2313479

I. Introduction

THE USE of energy-maximizing control has been accepted as crucial to the development of economic wave energy conversion [1]. The application of control to WECs allows the effective bandwidth of WECs to be increased, generating a near resonance condition at a wide range of wave frequencies. In general, WEC controllers can be separated into two hierarchical levels.

1) A high-level reference generation produces the optimum velocity profile for efficient energy extraction, which can also consider physical constraints on the system.
2) A low-level servo controller acts on the PTO force to impose the desired velocity profile from 1) on the system.

Such a hierarchical WEC control strategy has a strong analogy with wind turbine control systems, where the ideal rotor velocity is determined from optimal tip-speed considerations, with torque control then used to implement the reference rotor velocity. The overall structure of such hierarchical control schemes is depicted in Fig. 1.

Despite the prevalent use of linear models in WEC evaluation, simulation, and control [2], [3], there is an acknowledgment that such models are relatively simplistic in their representation of many nonlinear effects, including nonlinear Froude–Krylov forces [4], [5] and viscous drag forces [6], [7]. In particular, the concept of linearization around an equilibrium point (the zero displacement point) where operation is in the region of this equilibrium point is often violated, since the objective is to amplify the WEC motion (via resonance) in order to maximize energy capture. The achievement of resonance also produces large device velocities (particularly in large seas), resulting in significant viscous drag forces and vortex shedding. However, linear models are attractive due to intuitive connection with physical device quantities, their compact algebraic representation (permitting model-based control design), and their relatively low computational overhead.

An ideal situation, therefore, is that we utilize a linear model for WEC control, but address the issues associated with a lack of fidelity of the model for more significant device motion. This is addressed for the control structure in Fig. 1 as follows.

1) A reference generation controller is determined which is only weakly dependent on the WEC model.
2) A robust servo-controller is employed to address model uncertainty.

Such a concept has the advantages that the poor sensitivity and robustness properties of feedforward control (used in reference generation) are minimized, since the reference generation is only weakly dependent on the WEC model, whereas model

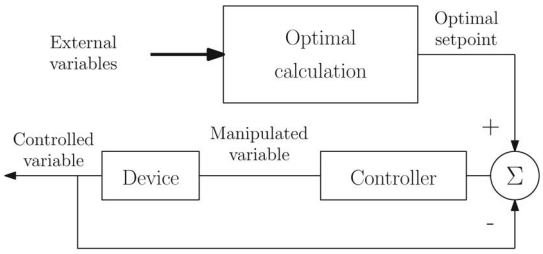

Fig. 1. Hierarchical control structure for wind turbines and wave energy devices.

uncertainties can be directly addressed using a robust feedback structure used to achieve the desired device velocity.

The reference-generation feedforward component was studied in [8]. This paper proposes two possibilities for the design of a robust feedback controller that deals with system nonlinearities. In the first approach, the nonlinearities are modeled as uncertainty bounds in the frequency domain and a linear controller is shaped based on the small-gain conditions for robust stability. The second approach is based on the concept of passivity and allows achieving robust stability as well as performance, without requiring a model of the nonlinearities. Although a less conservative nonlinear controller could be designed (e.g., by extending the linear model predictive control (MPC) designs proposed in [9]–[12]), an accurate model of the nonlinearity, for control purposes, is not always easy to obtain and model uncertainties are still present, in practical situations. In addition, nonlinear MPC controllers generally involve iterative calculations and the inclusion of a nonlinear model accentuates the convergence issues associated with WEC MPC controllers [12].

The remainder of the paper is laid out as follows. Section II develops the nonlinear WEC model, including the linear approximation for the nominal control design. In Section III, both feedforward (velocity reference) and feedback (velocity servo) controllers are detailed, with the investigations of two options for the design of the robust controller, to accommodate the linear model uncertainty. Section IV then documents a case study for a particular heaving buoy WEC operating in a irregular wave climate, showing the efficacy of the robust controller, whereas conclusions are drawn in Section V.

II. Model of the WEC

A. Hydrodynamic Model

We consider a single-body floating system oscillating in heave, as shown in Fig. 2. Energy is extracted from the relative motion with the sea bottom, through a generic PTO mechanism. The external forces acting on the WEC are the excitation from the waves and the control force produced by the PTO, namely $f_{\rm ex}(t)$ and $f_u(t)$. Additional hydrodynamic and hydrostatic forces arising due to the motion of the body in the water are the radiation force $f_r(t)$, the diffraction force $f_d(t)$, the viscous force $f_v(t)$, and the buoyancy $f_b(t)$ [3]. The equation of motion in one degree of freedom, excluding mooring forces, is specified as follows:

$$M\dot{v}(t) = f_r(t) + f_v(t) + f_b(t) + f_{ex}(t) + f_u(t) \qquad (1)$$

where $v(t)$ is the heaving velocity.

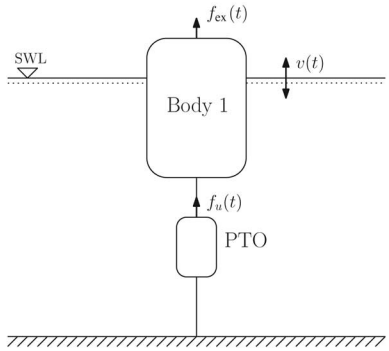

Fig. 2. One-degree of freedom floating system for wave energy conversion.

With the assumptions of linear potential theory [3], namely:
1) irrotational, incompressible, and inviscid fluid;
2) small-body approximation (wave elevation constant across the whole body);
3) small oscillations (constant wetted surface),

the following simplifying equations apply (more details in [3]):

$$f_{\rm ex} = \int_{-\infty}^{t} h_{\rm ex}(\tau)\eta(t-\tau)d\tau \qquad (2)$$

$$f_r(t) = -\int_{0}^{t} z_r(\tau)v(t-\tau)d\tau \qquad (3)$$

$$f_b(t) = -\rho g S_w \int_{0}^{t} v(\tau)d\tau \qquad (4)$$

$$f_v(t) = 0. \qquad (5)$$

In (2), the excitation (including diffraction) force is related to the incident wave $\eta(t)$ through the excitation kernel function $h_{\rm ex}(t)$. Equation (3) expresses the radiation force as a linear convolution of the radiation kernel $z_r(t)$ with the oscillation velocity. The buoyancy $f_b(t)$ models the hydrostatic equilibrium, related to the heaving position through a linear coefficient that depends on the gravity acceleration g, the water density ρ, and the surface area of the body cut by the mean water level S_w. Note the noncausality of the expression for the excitation force, where $h_{\rm ex}(t) \neq 0$ for $t \leq 0$ [3].

However, the assumptions of linear potential theory are not necessarily valid for oscillating WECs which are subject to significant motions around the mean water level. Several studies have been carried out in order to include quadratic terms of the fluid potential and the variations in time of the wetted surface [5], [13]. Simulation results clearly show how the linear model consistently overestimates the body motion, particularly in large waves. However, an explicit expression of the hydrodynamic forces that account for such nonlinearities has never been derived to date.

Another unacceptable assumption, in practical situations, is the absence of viscous forces. An experimental law was proposed by Morison [14]

$$f_v(t) = \rho R C_d |v(t)|v(t) + \rho\pi R^2 C_i \dot{v}(t) \qquad (6)$$

where ρ is the water density, R is the cylinder radius, C_d is the drag coefficient, and C_i is the inertia coefficient. Empirical validations of the Morison equation have proved its validity, and methods have been proposed to evaluate the coefficients C_d, C_i for certain specific shapes [6], [7].

A full nonlinear model of the WEC goes beyond the scope of this paper. For our study, we are going to assume that the nonlinearity of the system comes from the drag component of the viscous force, setting $C_i = 0$ [a nonzero C_i would only result in an additive constant to the mass M in (1)], without restricting the generality of our results. The heaving cylinder of Fig. 2 is, therefore, simulated by the following nonlinear model:

$$M\dot{v}(t) + \int_0^t z_r(\tau)v(t-\tau)d\tau + K_v|v(t)|v(t) + K_b\int_0^t v(\tau)d\tau = f_{\text{ex}}(t) + f_u(t) \tag{7}$$

where $K_v \triangleq \rho R C_d$ and $K_b \triangleq \rho g S_w$, and it is assumed that $v(t) = 0$ for $t \leq 0$.

B. Linear Model for Control Design

For convenience of control design, the force-to-velocity model of a WEC is typically expressed using a linear model in the frequency domain [3], [8]

$$\frac{V(\omega)}{F_{\text{ex}}(\omega) + F_u(\omega)} = \frac{1}{Z_i(\omega)} \triangleq P_n(\omega) \tag{8}$$

where $Z_i(\omega)$ is termed the intrinsic impedance of the system and $P_n(\omega)$ will be referred to as the nominal model. In (8), $V(\omega), F_{\text{ex}}(\omega)$, and $F_u(\omega)$ represent the Fourier transform of the velocity $v(t)$, excitation force $f_{\text{ex}}(t)$, and control force $f_u(t)$, respectively. Note that, in the following, unless stated otherwise, the Fourier transform of time-domain signals or functions will be denoted by the corresponding capital letter, namely $X(\omega) \triangleq \mathcal{F}\{x(t)\}$.

The intrinsic impedance $Z_i(\omega)$ of the model in (8) is specified as (refer to [3], [8] for the full derivation)

$$Z_i(\omega) = B(\omega) + K_v^{(0)} + j\omega\left[M + M_a(\omega) + M_\infty - \frac{K_b}{\omega^2}\right] \tag{9}$$

where $B(\omega)$ is the radiation resistance (real and even [3], [15]), $M_a(\omega) + M_\infty$ is the added mass (the constant term at infinite frequency M_∞ is separated to yield a well-define Fourier transform of $z_r(t)$ [3]), and $K_v^{(0)}$ is a linear damping coefficient approximating the nonlinear viscous damping in (7).

The model in (8) allows the derivation of conditions for optimal energy absorption and the intuitive design of the feedback controller in the frequency domain [3], [8]. Note that, of course, the controller can be designed directly from the nonlinear model. However, as specified in Section II-A, an explicit parametric nonlinear model is not attainable, in general. This study, therefore, shows how the simple design of the controller based on the linear model can be made robust to uncertainties stemming from unmodelled nonlinearities.

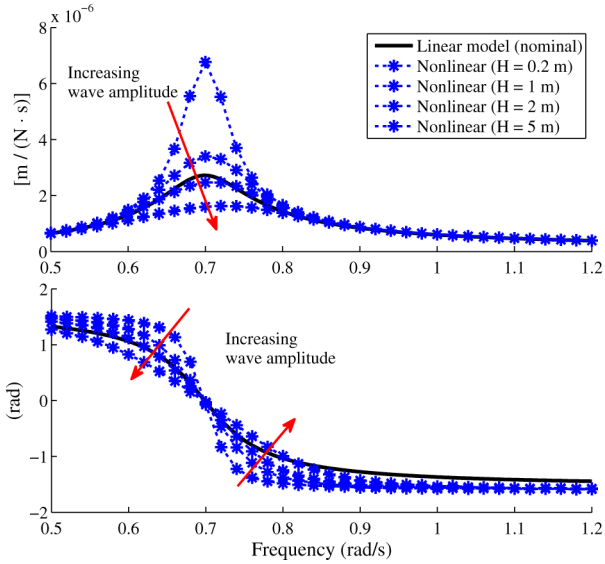

Fig. 3. Comparison between frequency response of linear system and nonlinear system at waves of different amplitudes.

The WEC system considered in this study consists of a heaving cylinder with radius $R = 7$ m, height $H = 20$ m, draught $h = 16$ m, and mass $M = 2.54 \times 10^6$ Kg. The radiation and excitation transfer functions $H_r(\omega)$ and $H_{\text{ex}}(\omega)$ are identified numerically through the hydrodynamic software Wamit [16]. The drag coefficient is set to $C_d = 1$, based on the numerical study in [6]. The linear viscous coefficient is set to $K_v^{(0)} = 3.17 \times 10^5$ Kg/s, such that the linear model is accurate when excited by waves of about 2 m in amplitude.

Fig. 3 compares the magnitude and phase response of the nonlinear model in (7), calculated with waves of different height and frequency, against the linear model in (8). The frequency response of the nonlinear system is evaluated in the sense of a describing function [17], as the complex amplitude-dependent ratio of the output fundamental to the input sinusoid, evaluated based on time-domain simulations.

III. Control System Design

The control system architecture is shown in Fig. 4 and was first introduced in [8], in the context of WECs. Based on the wave excitation force, a high-level controller calculates a reference velocity such that the energy absorption is maximized and the motion is within desired constraints. The velocity is then imposed on the WEC through a low-level feedback controller that acts on the PTO force.

Section III-A gives an overview of the high-level controller (the reader is referred to [8] for the full details). The design of the low-level controller, which is the main focus of this study, is then dealt with in Section III-B.

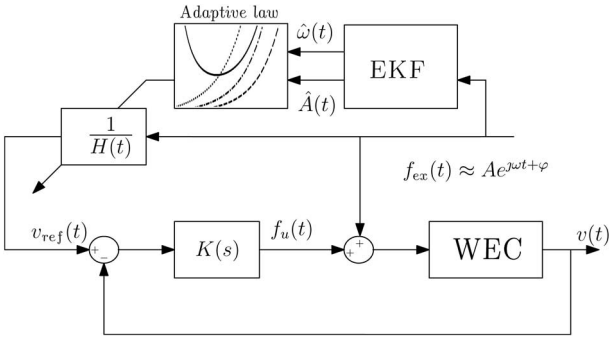

Fig. 4. Architecture of the hierarchical controller. The reference velocity is calculated by applying the adaptive gain $1/H(t)$ to the excitation force, based on (12).

A. High-Level Control

It is a well-known result that maximum wave power absorption from the WEC is achieved when [3]

$$V(\omega) = \frac{1}{2B(\omega) + 2K_v^{(0)}} F_{\rm ex}(\omega) \tag{10}$$

which gives the optimal amplitude and phase of the oscillating velocity in terms of the excitation force and the hydrodynamic properties of the system. However, noncausality [3], [15], [18] and excessive requirements in terms of motion/forces [3], [8], [9] make condition (10) impractical for many situations.

Based on the assumption that the wave excitation force is a narrow-banded harmonic process with a time-varying frequency $\omega(t)$ and amplitude $F_{\rm ex}(t)$, the reference velocity is calculated as a linear proportion of the wave excitation force

$$v_{\rm ref}(t) = \frac{1}{H(t)} f_{\rm ex}(t) \tag{11}$$

where $H(t)$ is adapted, online, according to the rule [8]

$$\frac{1}{H(t)} = \begin{cases} \frac{1}{2B(\omega)+2K_v^{(0)}}, & \text{if } \frac{\hat{\omega}X_{\rm lim}}{\hat{F}_{\rm ex}} > \frac{1}{2B(\omega)+2K_v^{(0)}} \\ \frac{\hat{\omega}X_{\rm lim}}{\hat{F}_{\rm ex}}, & \text{otherwise} \end{cases} \tag{12}$$

such that optimal power absorption is achieved, under the motion constraint $|x(t)| \leq X_{\rm lim}$ [8]. The estimation of $\hat{\omega}(t)$ and $\hat{F}_{\rm ex}(t)$ are obtained by use of the extended Kalman filter (EKF) applied to the true excitation force signal $f_{\rm ex}(t)$, assumed known [8], [18] (in practice, it would have to be estimated from motion and/or wave-elevation sensors).

The reference velocity, calculated from (11) and (12), is weakly dependent on the model of the system, which will result in close-to-optimal performance. In fact,

1) velocity and excitation force are always in phase, independent of the model;
2) the amplitude of the velocity is optimal in the constrained region, i.e., the second condition in (12), independent of the model;
3) in the unconstrained region, i.e., the first condition in (12), the amplitude of the velocity is suboptimal and depends on the approximation $2B(\omega) + 2K_v^{(0)}$.

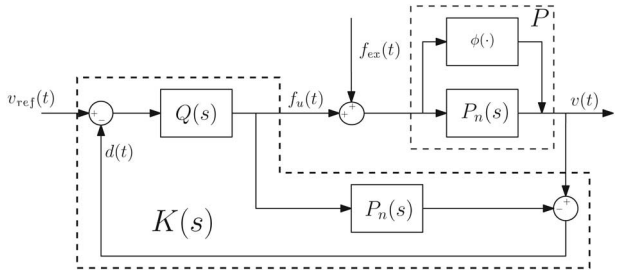

Fig. 5. IMC structure [19].

As already studied in [8], particularly in large waves (more of interest for energy extraction), WECs will mostly work in a constrained regime, so that the reference-generation strategy in (12) will only depend on the model for relatively small waves, where the linear model is more accurate. In this sense, we consider the proposed high-level controller to be weakly dependent on the model. Moreover, knowledge of the response of the nonlinear system at excitations of different magnitude could be incorporated in (12) to improve the accuracy of the amplitude relation, by adapting $K_v^{(0)}$ as a function of both $\hat{\omega}$ and $\hat{F}_{\rm ex}$, e.g., by means of a look-up-table and experimental data of the type shown in Fig. 3.

Note that alternative choices based, e.g., on modifications of the classical MPC [9]–[12] could be considered in the production of a velocity set-point, but these are not considered, here, since the focus of this paper is on the servo-controller loop.

B. Low-Level Feedback Control

The low-level servo controller is designed based on the principle of internal model control (IMC) [19], shown in Fig. 5. The feedback signal $d(t)$ can be interpreted as the difference between the output of the system P and the expected output based on the nominal model P_n. IMC exploits the idea that if a process and all its inputs are known perfectly, there is no need for feedback control or in other words that, for stable processes, feedback control is only needed because of uncertainty [19]. Note that IMC was already proposed in the context of wave energy [20], but the robust design was not explicitly addressed.

It can be easily shown [19] that the conceptual scheme in Fig. 5 is equivalent to the classical feedback loop of Fig. 4 when

$$K(s) = \frac{Q(s)}{1 - P_n(s)Q(s)}. \tag{13}$$

As is typical in control systems design, in (13) and in the following, $s \in \mathcal{C}$ denotes the complex frequency in the Laplace domain, on which transfer functions of finite-order linear systems are defined. The nominal model $P_n(s)$ is a finite-order approximation of $P_n(\omega)$, defined in (8), such that $P_n(s = j\omega) \approx P_n(\omega)$. The approximation is based on a finite-order approximation of the system radiation defined in [21] and more details can also be found in [8].

Although $K(s)$ is the actual feedback controller to be implemented in practice, the filter $Q(s)$ is the only design parameter of the IMC controller. Thanks to the special structure of IMC,

$Q(s)$ can be quite intuitively chosen, based on performance and robustness specifications, as will emerge in the following.

The relation between the output $v(t)$, the control input $v_{\text{ref}}(t)$, and the external excitation (disturbance) $f_{\text{ex}}(t)$ of the system in Fig. 5 is

$$\begin{aligned} v &= \frac{PQ}{1+Q(P-P_n)}v_{\text{ref}} + \frac{1-P_nQ}{1+Q(P-P_n)}Pf_{\text{ex}} \\ &= Tv_{\text{ref}} + SPf_{\text{ex}} \end{aligned} \tag{14}$$

where the dependence on the complex variable s has been dropped for brevity. The sensitivity function $S(s)$ and the complementary sensitivity function $T(s)$ are defined [19] as

$$S \triangleq \frac{1-P_nQ}{1+Q(P-P_n)} = \frac{v}{Pf_{\text{ex}}} \tag{15}$$

$$T \triangleq \frac{PQ}{1+Q(P-P_n)} = \frac{v}{v_{\text{ref}}}. \tag{16}$$

The sensitivity function expresses the response of the feedback system to the external disturbance. The complementary sensitivity indicates the tracking ability of the closed-loop system as well as the sensitivity to measurement disturbances [19]. When the plant coincides with the nominal model $P_n(s) = P(s)$, the ideal choice for $Q(s)$ is

$$\tilde{Q}(s) = P_n^{-1}(s) \tag{17}$$

such that perfect control is achieved: $S = 0$ (perfect disturbance rejection) and $T = 1$ (perfect reference tracking). However, the resulting $K = \tilde{Q}/(1 - P_n\tilde{Q})$ is not physically realizable, since $P_n(s)$ can be shown to be strictly proper, with relative degree 1, and nonminimum phase, with a zero at $s = 0$ [8], [15].

Therefore, the filter $Q(s)$ is augmented as

$$\tilde{Q}(s) = F(s)P_n^{-1}(s) \tag{18}$$

where $F(s)$ should be proper with relative degree of at least 1 and a zero at $s = 0$, in order to remove the unstable pole at $s = 0$ appearing from the inversion of $P_n(s)$. As already proposed in [8] and similarly in [20], $F(s)$ is designed as follows:

$$F(s) = \frac{s}{(s+0.2)} \cdot \frac{5}{s+5} \tag{19}$$

i.e., a band-pass filter which approximates perfect control in the frequency range [0.3, 2] rad/s (wave period of [21, 6.28] s). Note that this choice of $F(s)$ is somewhat arbitrary.

The controller thus-far obtained, namely $\tilde{K}(s)$, does not ensure closed-loop stability because the nominal model $P_n(s)$ is only a linear approximation of the actual behavior of the WEC. In the following, we investigate two approaches to adjust $\tilde{K}(s)$ such that the final controller $K(s)$ yields a robustly stable feedback loop.

1) Robustness Based on the Small-Gain Theorem: The following result, given in [19], can be conveniently utilized to derive a robust stability condition in terms of the filter $Q(s)$, by taking advantage of the IMC structure.

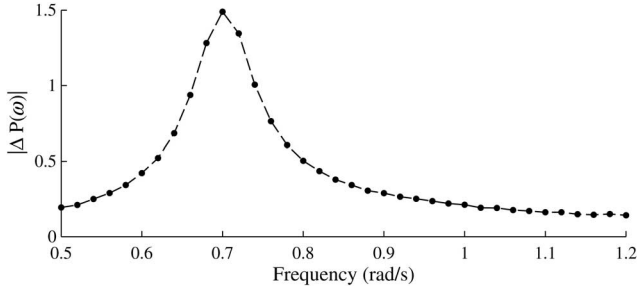

Fig. 6. Maximum relative uncertainty bound $\Delta P(\omega)$ for the nominal model with respect to the nonlinear system, as defined in (20).

Theorem 1: Assume that all the plants $P(s)$ in the family Π

$$\Pi = \left\{ P(s) : \frac{|P(j\omega) - P_n(j\omega)|}{|P_n(j\omega)|} \leq \Delta P(\omega) \right\} \tag{20}$$

have the same number of stable poles and that a particular controller $K(s)$ stabilizes the nominal plant $P_n(s)$. Then, the closed-loop system is robustly stable with the controller $K(s)$ if and only if the complementary sensitivity function for the nominal plant $T_n(s)$ satisfies the following condition:

$$||T_n(j\omega)\Delta P(\omega)||_\infty \triangleq \sup_\omega |T_n(j\omega)\Delta P(\omega)| < 1. \tag{21}$$

Proof: Immediate from the small-gain theorem [19]. □

Based on (16), the complementary sensitivity function for the nominal plant is $T_n(s) = Q(s)P_n(s)$ and robust stability is ensured if and only if

$$\sup_\omega |Q(j\omega)P_n(j\omega)\Delta P(\omega)| < 1. \tag{22}$$

By accounting for the nonlinearities as unstructured deviations from the nominal model, in the frequency domain, we can then make use of the result in Theorem 1. Fig. 6 shows $\Delta P(\omega)$ for the model given in Section II, calculated from time-domain simulations of the nonlinear model in (7) over a range of operating conditions, as given in Fig. 3. In practice, if a nonlinear model is not available, one may equally use physical wave-tank testing (by experimentally measuring the response of a prototype to sinusoidal waves) to produce an estimate of $\Delta P(\omega)$.

Fig. 7 shows how the initial $\tilde{Q}(s)$, given in (18), violates condition (21) at some frequencies and therefore, does not guarantees robust stability. The typical approach with IMC, as proposed in [19], is to augment the filter $Q(s)$ with an additional low-pass filter that rolls off the complementary sensitivity above a certain frequency. Usually, in fact, the uncertainty of a plant increases at high frequencies, due to unmodelled fast dynamics, and high complementary sensitivity at such frequencies is not required for performance.

In our case, however, the maximum uncertainty, as well as the violation of the condition for robust stability, is maximum around

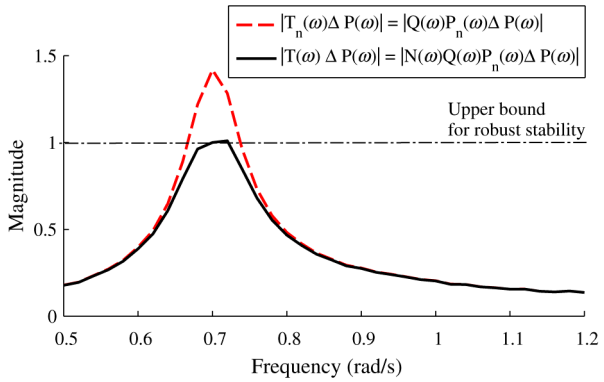

Fig. 7. Adjustment of the complementary sensitivity function, through a notch filter, for robust stability.

the center of the region (system resonance) where high complementary sensitivity would be desired, i.e., in the region [0.3, 2] rad/s. In order to achieve a better compromise between the drop in complementary sensitivity and improved robustness, the filter $Q(s)$ is, therefore, augmented with a notch filter, as also proposed in [22]

$$Q(s) = \tilde{Q}(s)N(s) \tag{23}$$

where

$$N(s) = \frac{s^2 + 2\beta\chi\omega_0 + \omega_0^2}{s^2 + 2\chi\omega_0 + \omega_0^2}. \tag{24}$$

In (24), ω_0 specifies the frequency of maximum attenuation (center of the notch), χ determines the bandwidth of the attenuation (width of the notch), and β is directly related to the maximum attenuation. Fig. 7 shows the effect of a choice of $\omega_0 = 0.7$ rad/s, $\beta = 1/1.42 \approx 0.71$ (peak variation of complementary sensitivity is nearly 1.42), and a bandwidth $\chi = 0.05$ (peak of uncertainty quite narrow). The resulting $T(s)$ satisfies the condition in (22) for robust stability.

The resulting controller is referred to as $K_{\mathrm{SG}}(s)$

$$K_{\mathrm{SG}}(s) = \frac{\tilde{Q}(s)N(s)}{1 - P_n(s)\tilde{Q}(s)N(s)}. \tag{25}$$

Although the proposed modification ensures robust stability, it also negatively affects tracking performance since a reduction in the complementary sensitivity causes an increase of the output sensitivity to the excitation force, as from (14). An alternative approach is investigated next, which allows us to safely address the robustness, while maintaining tracking performance.

2) Robustness Based on Passivity: An important result from input–output stability theory is the passivity theorem, stating that the feedback interconnection of a passive system and a strictly passive one is always input-output stable [23], [24].

Definition 1: A (possibly nonlinear) system $y(t) = f(\dot{y}, u, t)$ is passive if $\int_0^T y(t)u(t)dt \geq 0 \,\forall T \geq 0$ and for any $u(t)$.

Definition 2: A function of a complex variable $G(s)$ is positive real if $G(s)$ is analytic for $\Re\{s\} > 0$, $G(s)$ is real for real s, and $\Re\{G(s)\} \geq 0 \,\forall\, \Re\{s\} > 0$. We say that $G(s)$ is strictly positive real (SPR) if $\Re\{G(s)\} > 0 \,\forall \Re\{s\} > 0$.

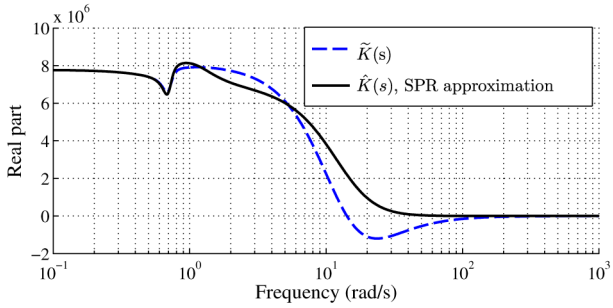

Fig. 8. SPR approximation of the nominal controller $\tilde{K}(s)$ based on (26).

A linear time-invariant system is (strictly) passive if its transfer function is (strictly) positive real [24].

Based on Definition 1, a passive system always dissipates energy (energy always positive). It can be immediately verified that the nonlinear model of the WEC, given in (7), is passive. The linear part of the system (radiation and buoyancy effects) is positive real [3], [21] and therefore passive, whereas the nonlinear viscous force in (6) is passive, since $f_v(t) \cdot v(t) > 0$ always. In addition, other nonlinear effects that may arise in the generic WEC model, given in (1), are all of a dissipative nature.

Based on the passivity theorem, it is therefore sufficient to design a SPR $K(s)$ in order to ensure closed-loop stability. Although it is difficult to approach the design of a controller with the SPR constraint, it is indeed possible to obtain a SPR approximation of an initial controller $\tilde{K}(s)$. In particular, the nominal controller obtained in (18) and (13) is approximated based on the procedure proposed in [24]

$$\hat{K}(s) = \arg\min \frac{1}{2\pi} \int_{-\infty}^{+\infty} |\tilde{K}(\jmath\omega) - K(\jmath\omega)|^2 d\omega$$
$$\text{subject to :} \quad K(s) \,\text{is SPR}. \tag{26}$$

The SPR constraint is formally expressed in terms of the coefficients of the denominator of the transfer function $K(s)$, and the problem in (26) is solved with nonlinear convex programming [24]. Fig. 8 compares the real parts of $\tilde{K}(s)$ (negative at times) and the resulting $K(s)$ (always positive).

Note that the design does not need any knowledge of the nonlinearity of the system, unlike the procedure proposed in Section III-B1. In addition, one can increase the gain of $K(s)$ while not worrying about the closed-loop stability (K is still SPR) and independently improve the reference-tracking and excitation-force-rejection properties of the servo controller. We apply an additional multiplicative gain of 20 to the final $K(s)$, based on intuitive design (the gain is increased until the velocity tracking is acceptable), as in Fig. 9. The resulting controller is referred to as $K_{\mathrm{SPR}}(s)$

$$K_{\mathrm{SPR}}(s) = 20\hat{K}(s). \tag{27}$$

Fig. 9 shows the superior velocity-tracking ability of K_{SPR} as opposed to K_{SG}. Also, note how increasing the closed-loop gain of K_{SG} leads to instability, whereas this is not true for K_{SPR}.

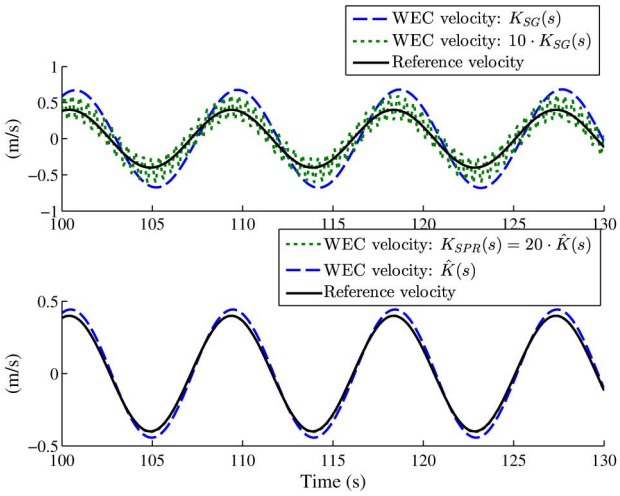

Fig. 9. Velocity tracking of $K_{\mathrm{SG}}(s)$ and $K_{\mathrm{SPR}}(s)$ when increasing gain. Reference velocity is a sinusoid with frequency 0.7 rad/s.

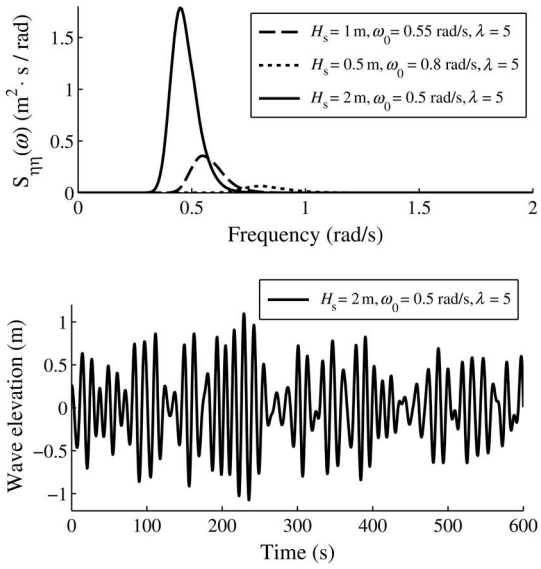

Fig. 10. Example of simulated waves. (a) Ochi spectral distributions [25]. (b) Time series simulated from the spectrum [26].

IV. Results

A. Wave Data

Simulation results are produced under several wave conditions. Random waves are generated from single-peaked, three-parameters Ochi spectral distributions [25]

$$S_{\eta\eta}(\omega) = \frac{\left(\frac{4\lambda+1}{4}\omega_0^4\right)}{\Gamma(\lambda)} \cdot \frac{H_s^2}{\omega^{4\lambda+1}} e^{-(4\lambda+0.25)(\omega_0/\omega)^4} \qquad (28)$$

where ω_0 is the peak frequency, H_s is the significant wave height, and λ is the sharpness.

The peak frequency is varied from 0.3 to 1.2 rad/s, with step 0.05, the significant wave heights are 0.5, 1, 2, and 4 m, and $\lambda = 5$ (not important for the purposes of this study; the reader may refer to [8] to verify how the bandwidth affects the high-level control strategy). Random-wave time-series of 7200 s, sampled at 2.56 Hz, are generated for each simulation, from $S_{\eta\eta}(\omega)$, based on the method proposed in [26] and also described in [8]. Fig. 10 gives an example of Ochi wave spectra and wave-elevation time-series.

B. Results

The performance of the hierarchical control system in Fig. 4 is evaluated across the range of waves described in Section IV-A, over which the linear model of WEC has a quite limited accuracy, as highlighted in Fig. 3. Two possible designs of a robust servo-controller are evaluated: 1) based on the small-gain theorem and on an unstructured frequency-bound model of the nonlinearity, named $K_{\mathrm{SG}}(s)$ and detailed in Section III-B1; and 2) based on the passivity theorem not requiring any knowledge of the nonlinearities, other than the assumption of their being dissipative (passive), named $K_{\mathrm{SPR}}(s)$, designed in Section III-B2, which is true in practice. As a comparison, we consider the nominal controller designed in Section III-B, denoted as $K_n(s)$, although this should not be implemented in practice, since it would cause instability.

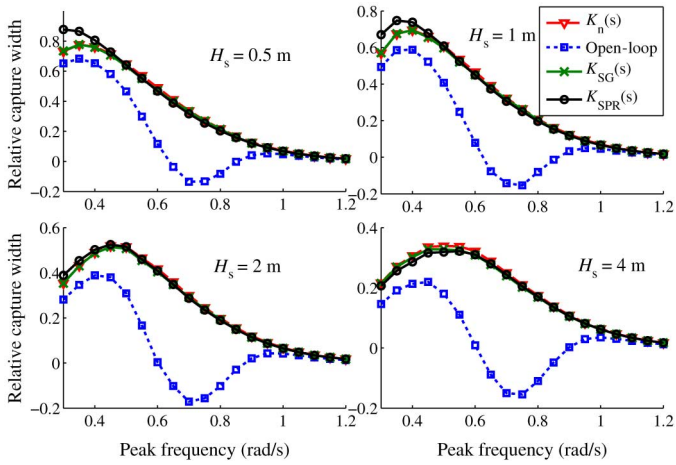

Fig. 11. Performance of the proposed robust controller against the open-loop controller based on the nominal model.

A first general measure of the robustness, shown in Fig. 11, is the overall energy extraction, in terms of RCW [8], obtained by the controllers over the whole range of wave conditions. Clearly, the open-loop nominal controller produces unwanted results (negative energy extraction) over a wide range of frequencies around resonance (0.7 rad/s), where the largest model uncertainty is. Both of the proposed servo-controller, on the other hand, are clearly robust in all sea conditions, producing the expected RCW. $K_{\mathrm{SPR}}(s)$ is seen to be superior, particularly for low-frequency waves, and this is due to the superior velocity-tracking performance, highlighted in Section III-B. Fig. 12 shows how the actual velocity produced by $K_{\mathrm{SG}}(s)$ is not quite in phase with the desired velocity, which is the main cause for its lower performance, in terms of energy capture.

The root-mean-square error (RMSE) between the reference velocity and the actual velocity is shown in Fig. 13, and the superior performance of the controller based on passivity is even

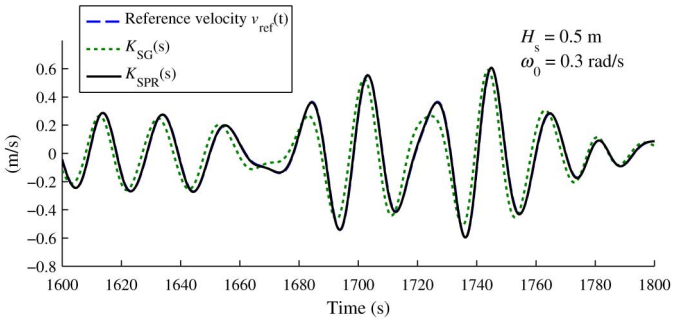

Fig. 12. Example of velocity-tracking performance of proposed controllers. Note that $v_{\mathrm{ref}}(t)$ is indistinguishable from the velocity produced by $K_{\mathrm{SPR}}(s)$.

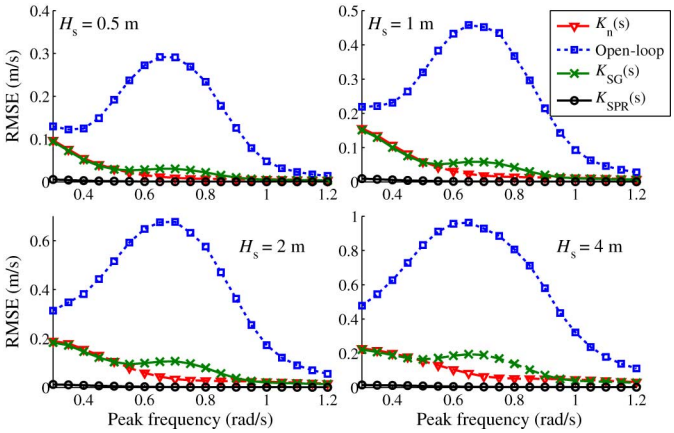

Fig. 13. RMSE between actual velocity and reference velocity with the different proposed controllers.

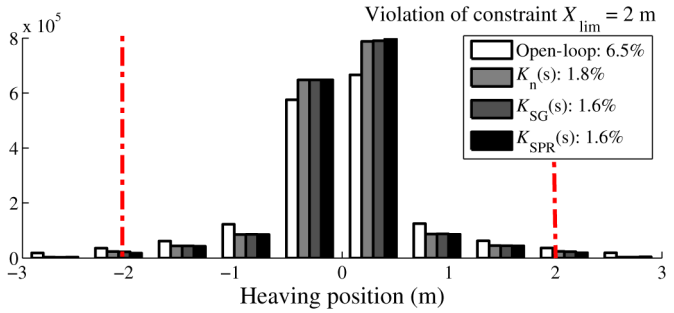

Fig. 14. Distribution of the WEC heaving position with the different proposed controllers.

more evident. The gain of $K_{\mathrm{SPR}}(s)$ can, in fact, be increased without affecting the closed-loop stability so that the controller is much faster in responding to the changes in reference velocity.

The importance of accurately following the desired reference velocity is not only evident in the energy-capture performance of the WEC, but also in the ability to satisfy the desired motion constraints. The proposed strategy for the generation of the velocity setpoint, given in (12), also accounts for the motion constraint $X_{\mathrm{lim}} = \pm 2$ m. Fig. 14 shows the distribution of the heaving position over the whole range of proposed simulations. The given constraint is exceeded about 6.5% of the times with the open-loop nominal controller, whereas less than 2% of the times with the proposed robust controllers. Given the very accurate reference-tracking performance of the controller $K_{\mathrm{SPR}}(s)$, in particular, such constraint violations are mostly due to the monocromatic time-varying approximation of key system variables and instantaneous frequency/amplitude estimations of the high-level controller, already discussed in [8].

V. Conclusion

This paper addresses realistic control of wave energy devices. We have attempted to find a sensible tradeoff between performance and simplicity, resulting in a fixed parameter controller with no requirement for wave forecasting, while directly addressing linear modeling errors due to nonlinear viscosity effects. The design procedure is both intuitive and straightforward, with no requirement for numerical optimization; yet, physical system constraints can be directly addressed. Although the performance of the resulting controller is sub-optimal, with some conservatism due to the robust formulation, we feel that the performance penalty over a nonlinear controller which deals explicitly with system nonlinearities is more compensated by the linear controller simplicity.

References

[1] M. T. Pontes and A. Brito-Melo, "International energy agency cooperate R&D on ocean energy," in *Proc. 5th Eur. Wave Energy Conf.,* Cork, Ireland, 2003, pp. 10–13.

[2] J. Cruz, *Ocean Wave Energy: Current Status and Future Perspectives.* Berlin, Germany: Springer-Verlag, 2008.

[3] J. Falnes, *Ocean Waves and Oscillating Systems.* Cambridge, U.K.: Cambridge Univ. Press, 2002.

[4] J.-C. Gilloteaux, "Mouvements de grande amplitude d'un corps flottant en fluide parfait. Application à la récupération de l'énergie des vagues," Ph.D. dissertation, Ecole Centrale de Nantes, France, 2007.

[5] A. Merigaud, J.-C. Gilloteaux, and J. V. Ringwood, "A nonlinear extension for linear boundary element methods in wave energy device modelling," in *Proc. 31st Int. Conf. Ocean Offshore Arctic Eng.* (OMAE), Rio de Janeiro, Brazil, 2012, pp. 615–621.

[6] M. A. Bhinder, A. Babarit, L. Gentaz, and P. Ferrant, "Assessment of viscous damping via 3D-CFD modelling of a floating wave energy device," in *Proc. 9th Eur. Wave Tidal Energy Conf.* (EWTEC), Southampton, U.K., 2011.

[7] Z. Yuan and Z. Huang, "An experimental study of inertia and drag coefficients for a truncated circular cylinder in regular waves," *J. Hydrodyn.*, vol. 22, no. 5, pp. 318–323, 2010.

[8] F. Fusco and J. V. Ringwood, "A simple and effective real-time controller for wave energy converters," *IEEE Trans. Sustain. Energy*, vol. 4, no. 1, pp. 21–30, Jan. 2013.

[9] J. Hals, J. Falnes, and T. Moan, "Constrained optimal control of a heaving buoy wave-energy converter," *J. Offshore Mech. Arctic Eng.*, vol. 133, no. 1, p. 011401, 2011.

[10] G. Bacelli, J. V. Ringwood, and J.-C. Gilloteaux, "A control system for a self-reacting point absorber wave energy converter subject to constraints," in *Proc. 18th Int. Fed. Autom. Control World Congr.* (IFAC), Milano, Italy, 2011, pp. 11 387–11 392.

[11] J. A. M. Cretel and G. Lightbody, "Maximisation of energy capture by a wave-energy point absorber using model predictive control," in *Proc. 18th Int. Fed. Autom. Control World Congr.* (IFAC), 2002, Milano, Italy, 2011, pp. 3714–3721.

[12] M. Richter, M. E. Magaña, S. Member, O. Sawodny, and T. K. A. Brekken, "Nonlinear model predictive control of a point absorber wave energy converter," *IEEE Trans. Sustain. Energy*, vol. 4, no. 1, pp. 118–126, Jan. 2013.

[13] J.-C. Gilloteaux, G. Bacelli, and J. V. Ringwood, "A non-linear potential model to predict large-amplitudes-motions: Application to a multi-body wave energy converter," in *Proc. 10th World Renew. Energy Congr.* (WREC'10), Glasgow, Scotland, 2010, pp. 934–939.

[14] J. R. Morison, M. P. O'Brien, J. W. Johnson, and S. A. Schaaf, "The force exerted by surface waves on piles," *AIME Petrol. Trans.*, vol. 189, pp. 149–154, 1950.
[15] F. Fusco and J. V. Ringwood, "A study on the prediction requirements in real-time control of wave energy converters," *IEEE Trans. Sustain. Energy*, vol. 3, no. 1, pp. 176–184, Jan. 2012.
[16] Wamit Inc., MA, *WAMIT Version 6.4,* 2008.
[17] D. Atherthon, *Nonlinear Control Engineering.* New York, NY, USA: Van Nostrand Reinhold, 1982.
[18] F. Fusco and J. V. Ringwood, "Short-term wave forecasting for real-time control of wave energy converters," *IEEE Trans. Sustain. Energy*, vol. 1, no. 2, pp. 99–106, Jul. 2010.
[19] M. Morari and E. Zafiriou, *Robust Process Control.* Englewood Cliffs, NJ, USA: Prentice-Hall, 1989.
[20] J. Sá da Costa, P. Beirão, and D. Valério, "Internal model control applied to the archimedes wave swing," in *Proc. 16th Int. Conf. Control Syst. Comput. Sci.* (CSCS), Bucharest, Romania, 2007.
[21] T. Perez and T. I. Fossen, "A MATLAB toolbox for parametric identification of radiation-force models of ships and offshore structures," *Model Identif. Control*, vol. 30, no. 1, pp. 1–15, 2009.
[22] H. Procházka and I. D. Landau, "Pole placement with sensitivity function shaping using 2nd order digital notch filters," *Automatica*, vol. 39, no. 6, pp. 1103–1107, Jun. 2003.
[23] C. A. Desoer and M. Vidyasagar, *Feedback Systems: Input-Output Properties.* New York, NY, USA: Academic, 1975.
[24] C. Damaren, H. Marquez, and A. Buckley, "Optimal strictly positive real approximations for stable transfer functions," *IEE Proc. Control Theory Appl.*, vol. 143, no. 6, pp. 537–542, Nov. 1996.
[25] M. K. Ochi and E. N. Hubble, "Six-parameter wave spectra," in *Proc. 15th Int. Conf. Coastal Eng.,* 1976, pp. 301–328.
[26] J. Figwer, "A new method of random time-series simulation," *Simul. Pract. Theory*, vol. 5, pp. 217–234, 1997.

Francesco Fusco (S'09–M'11) received the master degree in industrial automation engineering from Università Politecnica delle Marche (UNIVPM), Ancona, Italy, in 2008, and the Ph.D. degree in electronic engineering from the National University of Ireland (NUI), Maynooth, Ireland, in 2012.

Since 2012, he has been a Research Scientist with the Smarter Cities Technology Centre, IBM Research, Ireland.

Mr. Fusco is a Chartered Engineer in Italy.

John V. Ringwood (M'87–SM'97) received the diploma degree in electrical engineering from Dublin Institute of Technology, Dublin, Ireland, and the Ph.D. degree in control systems from Strathclyde University, Glasgow, U.K., in 1981 and 1985, respectively.

He is currently a Professor of electronic engineering with the National University of Ireland (NUI), Maynooth, Ireland, and Associate Dean for engineering with the Faculty of Science and Engineering. From 2000 to 2005, he was the Head of the Electronic Engineering Department, NUI Maynooth, developing the Department from a greenfield site. His research interests include time series modeling, wave energy, control of plasma processes, and biomedical engineering, and he currently directs the Centre for Ocean Energy Research, NUI Maynooth.

Dr. Ringwood is a Chartered Engineer and a Fellow of the Institution of Engineers of Ireland.